

The effect of scan pattern on microstructure evolution and mechanical properties in electron beam melting Ti47Al2Cr2Nb

Wenjun Ge^{1, 2, 3}, Feng Lin^{1, 2, 3}, Chao Guo^{1, 2, 3}

1. Department of Mechanical Engineering, Tsinghua University, Beijing 100084;
2. Key Laboratory for Advanced Materials Processing Technology, Ministry of Education of China, Tsinghua University, Beijing 100084;
3. Biomanufacturing and Rapid Forming Technology Key Laboratory of Beijing, Tsinghua University, Beijing 100084.

REVIEWED

Abstract

Ti47Al2Cr2Nb alloy square samples with dimensions of 20mm×20mm×5mm were fabricated by electron beam selective melting. In order to study the effect of electron beam scan pattern on the microstructure evolution, three different scan patterns were employed: S-shaped scan line, Z-shaped scan line and interlayer orthogonal S-shaped scan line. Microstructural and chemical analyses were conducted using optical microscopy, scanning electron microscopy and energy differential system. It is worth noting that the element Al loss rate was about 8% under different process parameters. As a result, the microstructures of EBSM Ti47Al2Cr2Nb samples were composed of columnar β grains, α/α_2 and α_2/γ lamellar. Tensile tests were carried out to understand the mechanical properties to the corresponding microstructures. Ultimate Tensile Stress (UTS) at room temperature is much lower than that at a high temperature.

Introduction

Intermetallic TiAl alloys are gaining more and more attentions because of the outstanding properties such as the low density (3.9-4.2g.cm⁻³), high strength and high-temperature oxidation and creep resistance. TiAl alloys appear as promising high-temperature materials used in automotive, energetic and aerospace industries. However, TiAl alloys exhibit poor processing plasticity at room temperature which

leads to poor workability at room temperature. Recently, electron beam selective melting (EBSM) has been studied as a feasible method for manufacturing Ti6Al4V and Ti-Al intermetallic [1-3]. Electron beam selective melting is one of the additive manufacturing methods with high fabrication quality. Compared to laser manufacturing [4], electron beam selective melting has higher energy density and scan speed which reduce the time and cost of manufacturing. In addition, EBSM technology has advantages of vacuum fabrication environment in fabricating impurity sensitive and highly reflective materials. Therefore it is of particular interest to investigate the EBSM fabrication of intermetallic TiAl components.

TiAl alloys have four typical microstructures and the mechanical properties of TiAl alloys are strongly dependent on the microstructure. In electron beam selective melting, columnar crystals trend to be formed because of the high cooling rate and big temperature gradient. The scan pattern has an effect on the temperature gradient, which would further influence the growth of grains and the mechanical properties. This work investigated the microstructures and resultant mechanical properties of samples fabricated employing three different scan patterns, namely S-shaped scan line, Z-shaped scan line and interlayer orthogonal S-shaped scan line (also called interlayer cross scan line).

Experiments

In this study, square samples were fabricated by electron beam selective melting from pre-alloyed Ti47Al2Cr2Nb powders with particle sizes between 45 and 150 μm (Fig.1). The powder had a chemical composition (in atomic percentage) of 46.51% aluminum, 0.02% niobium, 0.02% chromium, balance titanium. The powder exhibits fine surface and highly spherical shape, and little satellite particles are also visible.

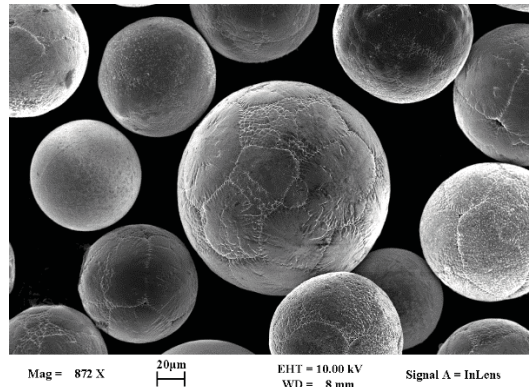


Fig.1 microscopic view of Ti47Al2Cr2Nb powder

Fig.2 shows the schematic diagram of EBSM-250 system designed by Tsinghua University. Compared with commercial EBSM equipment, EBSM-250 system can mix two kinds of powder together and then fabricate functionally gradient materials. In the system, electron beam is generated in the electron gun and accelerated at a voltage of 60KV. The electron beam is focused by focusing coil and scanned by deflection coil to preheat and selectively melt powders layer-by-layer.

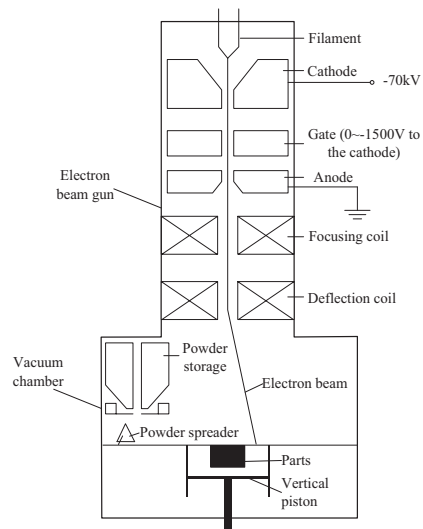


Fig.2 schematic diagram of EBSM-250 system designed by Tsinghua University

In this work, a preheating beam current of 20mA, a melting beam current of 6mA a hatching distance of 0.1mm and a scan speed of 0.2m/s were employed. Components were built directly on 316L stainless steel base plate dimensioning 10mm in thickness and 90mm×90mm in area. Before fabrication, the stainless steel base plate was preheated to about 800°C. The effect of scan pattern on microstructure and mechanical properties were investigated systematically by varying the scan

pattern. The three scan patterns used are shown schematically in Fig.3.

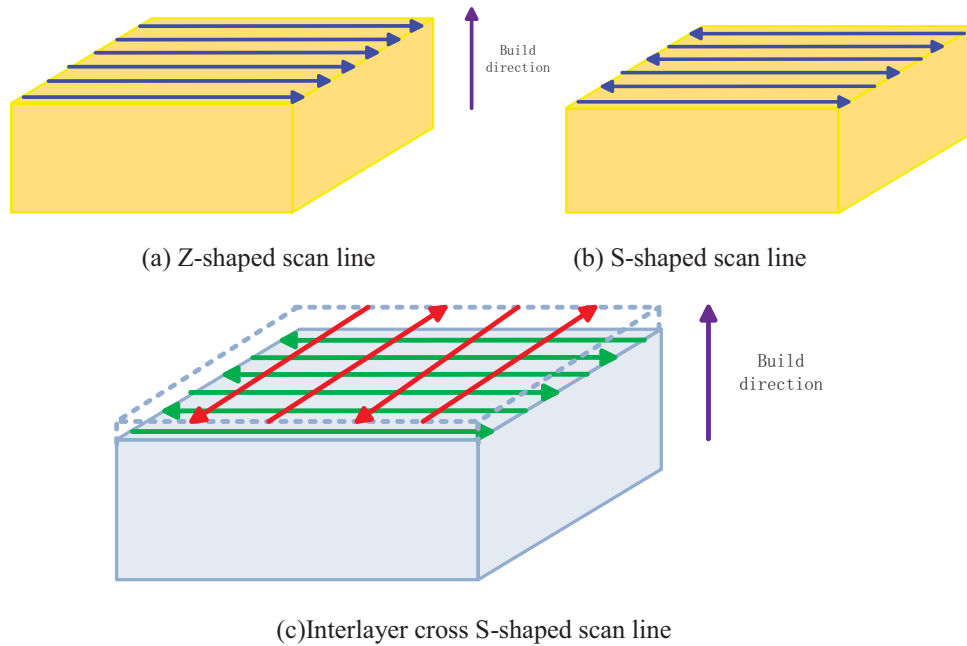


Fig.3 Scan patterns used in EBSM process

The fabricated specimens were cut along the deposition direction employing electron-discharge machining and then mounted, ground, polished and etched. Kroll's reagent was used to etch the samples. The microstructure of EBSM samples was characterized using optical microscopy and scanning electron microscopy. Crystallographic orientation was examined by electron backscattered diffraction (EBSD). Flake samples were taken for tensile tests at different temperatures on a universal material tension machine.

Results and discussion

3.1 Aluminum loss

As reported before, element Al loss is dependent on energy input and beam current. High energy input and beam current will result in high loss rate. Carolin Korner^[5] found that line energy of 1.1J/mm and beam current of 9.2mA cause a Al loss of about 4% while line energy of 0.7J/mm and beam current of 3.5mA reduce the loss to about 1at.%. Denis Cormier et al^[6] fabricated Ti-47Al-2Cr-2Nb samples employing a scan speed of 0.1m/s and a beam current of 13mA, and found approximately 6.1%

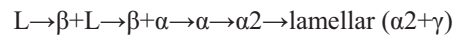
of the aluminum vaporized during the process. In this paper, specimens were fabricated employing a beam current of 6mA, a scan speed of 0.1m/s and a layer thickness of 0.1mm under three different scan patterns. Energy-dispersive spectroscopy (EDS) was employed to conduct the element analyses and the results are shown as Table-1. After the comparison with the original atomic percentage of the powder, it is demonstrated that the element loss rate of Al varies from 8% for S-shaped scan line to 6% for Z-shaped scan line.

Table-1 Element analyses results (at. %)

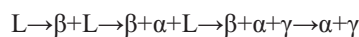
	S-shaped	Cross S-shaped	Z-shaped
Al	38.15	39.20	40.13
Ti	57.32	56.16	55.32
Cr	1.58	1.76	1.65
Nb	2.95	2.88	2.90

The formation and transformation of the microstructure are strongly influenced by Al loss, especially high losses. In light of the Ti-Al two-phase diagram, the solidification reactions altered significantly with the percentage of Al.

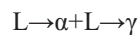
(1) Al < 42 at. %



(2) 42 at. % < Al < 50 at. %



(3) 42 at. % < Al < 50 at. %



Previous investigations reveal that the processing parameters have a remarkable influence on Al loss. Further investigation is needed to adjust the energy input to avoid over-heating and reduce Al evaporation.

3.2 Microstructure evolution

Microstructure evolution is closely related to the cooling and heating history during the process. EBSM process has a characterization of rapid solidification and

repeated heat cycling. In general, the microstructures of EBSM fabricated Ti47Al2Cr2Nb alloy consist of highly columnar prior β grain along the building direction and α_2 plates. As the composition varies during the EBSM process, the microstructures of EBSM fabricated Ti47Al2Cr2Nb alloy consist of highly columnar β grain along the building direction, α' , α_2 and $\alpha_2+\gamma$ lamellar.



(a) Cross scan



(b)S-shaped scan



(c)Z-shaped scan

Fig.4 optical microscopic photo of samples

The dendritic crystal growth develops in a positive temperature gradient. The formation of columnar prior β grains is a result of thermal gradient in the building direction. Many researchers [7-9] reported such columnar microstructures in the additive laser manufacturing (ALM) and EBSM of Ti6Al4V and Nickel-base super alloy. Components fabricated by EBSM are surrounded by loose powders which act as thermal insulation while the base plate and deposited materials act as heat dissipation parts. Due to this gradient, a preferred orientation of the dendrites in the forms of arrays with a typical spacing is obtained. For β grains, a body-centered cubic crystal, the [100] is the preferential crystallization direction. The elongated grains grow towards the molten pool and tilt a certain angle to the Z-direction. As shown in Fig.5, the EBSD pattern results also reveal the columnar preferred orientation. As the interlayer cross S-shaped scan line leads to the deviation of the direction of the temperature gradient, the growth of columnar crystal were interrupted. Fig.4(a) shows the optical microscopy of Cross-shaped scan specimen, the main structure is still columnar grains which is parallel to the building direction. Compared to the S-shaped scan specimen, the size of columnar β grain of Cross-shaped decrease from 400 μm to \sim 200 μm and the grains become more equiaxed.

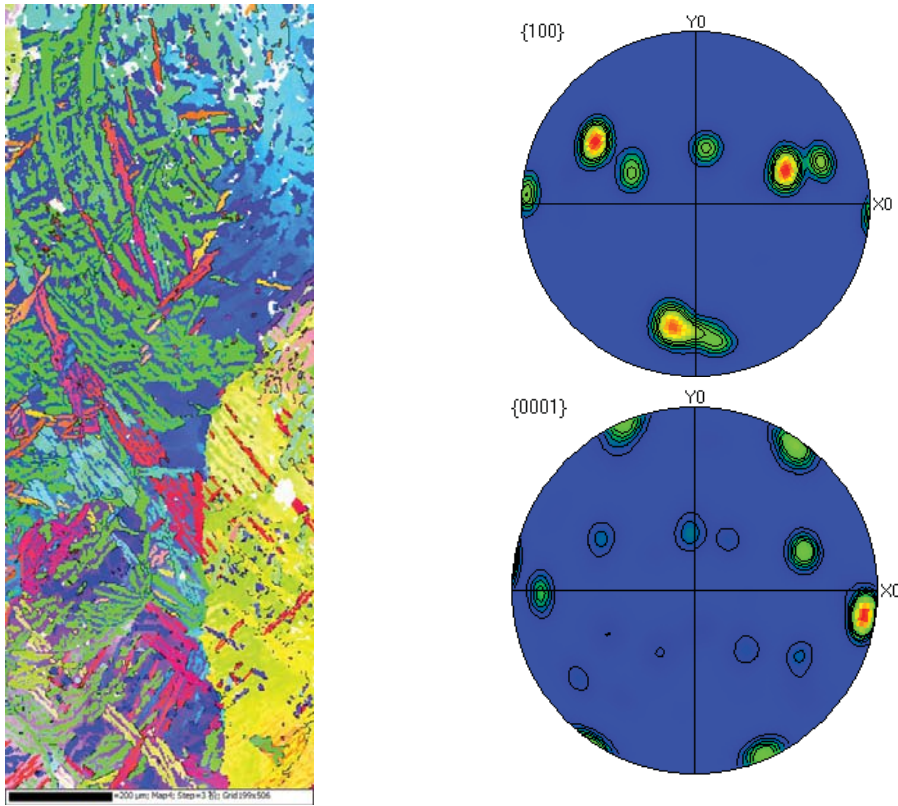
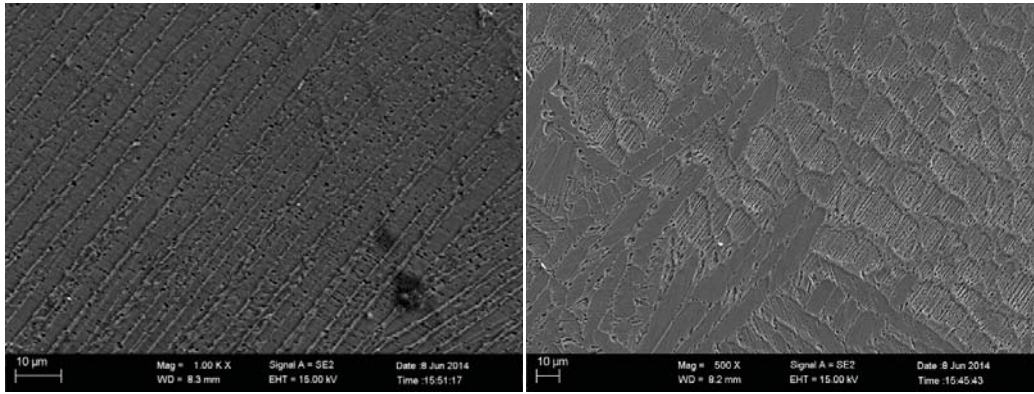


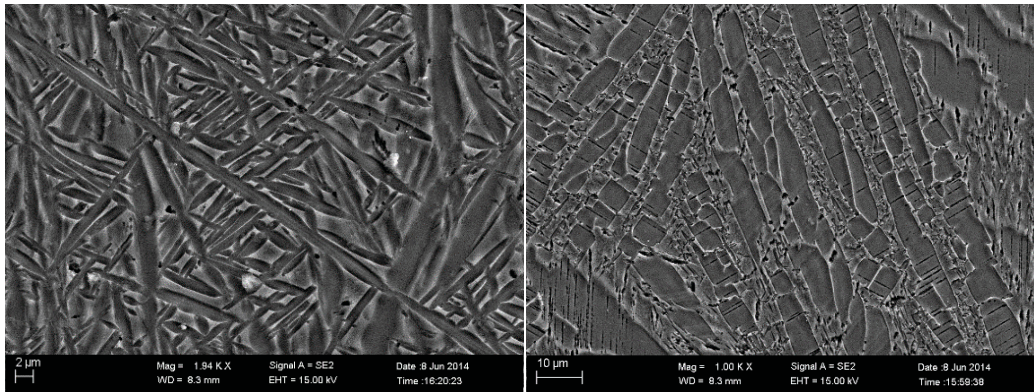
Fig.5 Orientation image and Pole figure of Cross-scan Ti47Al2Cr2Nb alloy

Fig.6 (a), (c), (e) show the microstructures obtained using the three different scan pattern. A thin layer $\sim 1\text{mm}$ of martensite α phase is observed at the top of the sample as a result of high cooling rates. Qian et al^[10] and S.S. AL-BERMANI^[11] reported that the cooling rate of top layer from liquid was $\sim 7 \times 10^4 \text{K} \cdot \text{s}^{-1}$ and $10^3 \sim 10^5 \text{K} \cdot \text{s}^{-1}$ in SLM and EBM Ti6Al4V. Although the exact cooling rate of Ti47Al2Cr2Nb is unknown, cooling rate of the new deposited layer is high enough to get martensite α . As samples increase in height, the temperature of the deposited layers are kept in relative high temperature and transformation $\alpha \rightarrow \alpha_2$, $\alpha_2 \rightarrow \alpha_2 + \gamma$ take place. Fig6 (b), (d), (f) show the basket weave/ Widmanstatten α/α_2 laths and α_2/γ lamellar in the middle of the samples. In the middle and bottom of the samples coarsen α can be observed with width of $\sim 5\mu\text{m}$. The form of coarse α lath is influenced by thermal cycling during the new deposited layers. Deposited part of the samples was kept in a relatively high temperature, for SLM Ti6Al4V the temperature is

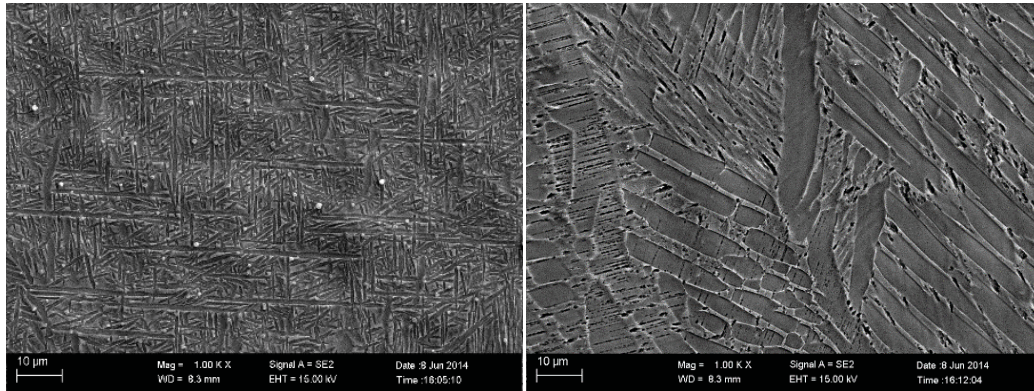


(a) top of Cross-scan

(b) middle of cross scan



(c) top of S-scan (d) middle of S-scan



(e) top of Z-scan (f) middle of Z-scan

Fig.6 SEM photos of samples

3.3 Tensile Test

Tensile specimens were tested on an Instron-5967 tensile machine using special grips at an engineering strain rate of $2 \times 10^{-4} \text{ s}^{-1}$. Tensile properties at room temperature and the high temperature of 700°C are illustrated in Fig.7. Fig.8 shows the fracture surface features for the S-shaped scan specimens at room temperature and the high temperature. Translamellar fracture appears to be the major failure mode in the two

samples at different temperatures. The UTS at 700°C is dramatically enhanced. The tensile strength at the room temperature of Cross-scan and S-scan samples is 271.3MPa and 362.6MPa, while the tensile strength at the high temperature is 679MPa and 769.6MPa respectively. The reason may be that specimens for high temperature test experienced a short time(5min) of heat preservation process which has a certain effect on reducing the residual stress. During the additive manufacturing process, repeated heating and cooling cycles in the material induce important thermal gradients and then may cause residual stress in samples after process. Many researchers [12-13] investigated the residual stress in selective laser melting process and the results show that the main residual stress is tensile stress. The exist of tensile stress in the specimens may decrease room temperature tensile strength.

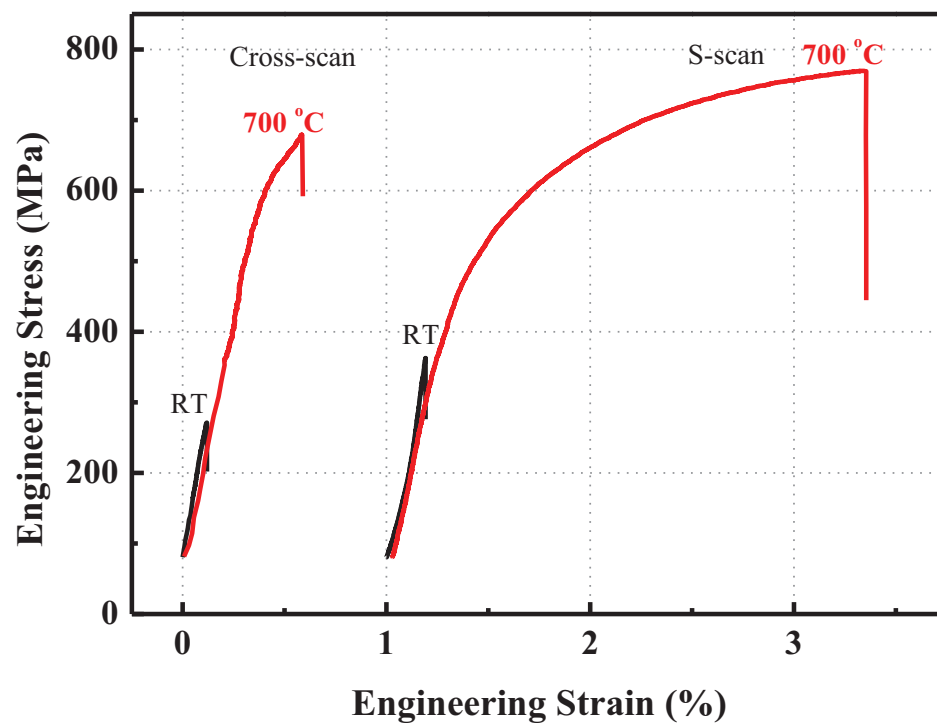
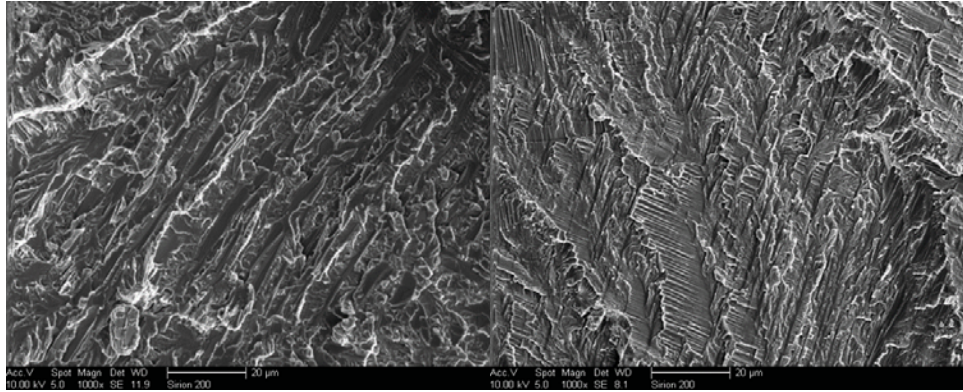


Fig.7 the tensile curves of different samples at different temperatures



(a) Room Temperature

(b) 700 °C

Fig.8 S-shaped scan sample fracture surface features

Conclusions

Ti47Al2Cr2Nb alloy square samples were fabricated by electron beam selective melting from pre-alloyed powders. The scan pattern has an effect on the temperature gradient, which would further influence the growth of grains and the mechanical properties. In order to study the effect of electron beam scan pattern on the microstructure evolution, three different scan patterns were employed: S-shaped scan line, Z-shaped scan line and interlayer orthogonal S-shaped scan line.

The element analyses by EDS demonstrated that the element loss rate of Al ranged from 6at. % to 8at. % employing different scan patterns. According to the Ti-Al two-phase diagram, the microstructures of EBSM Ti47Al2Cr2Nb samples were composed of columnar β grains, α/α_2 and α_2/γ lamellar. The dendritic crystal growth develops along the direction of heat dissipation, which is influenced by scan patterns. As the interlayer cross S-shaped scan line leads to the deviation of the direction of the temperature gradient, the growth of columnar crystal were interrupted. Therefore the size of the columnar crystal in cross-scanned specimens appeared smaller than the others.

Tensile tests at room temperature and high temperature of 700 °C were carried out to understand the mechanical properties to the corresponding microstructures. At the room temperature, the specimens employing interlayer cross S-shaped scan line achieve an ultimate tensile stress (UTS) of 271.3MPa, while the UTS of the

specimens employing S-shaped scan line is 362.6MPa. It is worth noting that UTS at the temperature of 700°C is much higher, 679MPa and 769.6MPa for cross scan and S-shaped scan respectively.

Acknowledgements

This work has been supported by the funding of 2013 Beijing Science and Technology Development Project, project numbers D13110400300000 and D131100003013002.

References

[1] Denis Cormier, Ola Harrysson, Tushar Mahale, Harvey West. Freeform Fabrication of Titanium Aluminide via Electron beam Melting Using Prealloyed and Blended Powders. Research Letters in Materials Science, Volume 2007.

[2] L.E.Murr, E.V.Esquivel, S.A. Quinones, et al. Microstructures and mechanical properties of electron beam-rapid manufactured Ti-6Al-4V biomedical prototypes compared to wrought Ti-6Al-4V. Materials characterization 60(2009)96-105.

[3] Luca Facchini, Alberto Molinari. Microstructure and mechanical properties of Ti-6Al-4V produced by electron beam melting of pre-alloyed powders. Rapid Prototyping Journal 15/3(2009)171-178.

[4] Lawrence E. Murr, Sara M. Gaytan, Diana A. Ramirez, et al. Metal Fabrication by Additive Manufacturing Using Laser and Electron Beam Melting Technologies. Mater. Sci. Technol., 2012, 28(1), 1-14.

[5] Selective electron beam melting of Ti-48Al-2Nb-2Cr, Jan Schwerdtfeger, Carolin Korner, Intermetallics, 49(2014)29-35.

[6] Freeform Fabrication of Titanium Aluminide via Electron Beam Melting Using Prealloyed and Blended Powders, Research Letters in Materials Science, Volume 2007.

[7] L.E. Murr, E. Martinez, S.M. Gaytan, et al. Microstructural Architecture,

Microstructures, and Mechanical Properties for a Nickel-Based Superalloy Fabricated by Electron Beam Melting. Metallurgical and Materials Transactions A, Volume 42A, November 2011-3491.

[8] H.K. Rafi, N.V. Karthik, Haijun Gong, et al. Microstructures and Mechanical Properties of Ti6Al4V Parts Fabricated by Selective Laser Melting and Electron Beam Melting. Journal of Material Engineering and Performance, Volume 22(12) December 2013.

[9] Shi-Hai Sun, Yuichiro Koizumi, Shingo Kurosu, et al. Build direction dependence of microstructure and high-temperature tensile property of Co-Cr-Mo alloy fabricated by electron beam melting. Acta Materialia 64(2014)154-168.

[10] Qian et al, Thermal history and microstructure of direct laser fabricated Ti-6Al-4V. Material Science and Technology, Vol21,2005.

[11] S.S. Al-bermani, M.L. Blackmore, W.Zhang and I.Todd. The origin of microstructural diversity, texture, and mechanical properties in electron beam melted Ti-6Al-4V. Metallurgical and Materials Transaction A, Volume 41A, December 2010.

[12] B. Vrancken, R. Wauthle, J.-P.Kruth, J.Van Humbeeck. Study of the influence of material properties on residual stress in selective laser melting.

[13] Peter Merceies and Fean-Pierre Kruth. Residual stresses in selective laser sintering and selective laser melting. Rapid Prototyping Journal, 12/5(2006) 254-265.